Crystal Structure and Magnetic Properties of $MnCu(obbz)(H_2O)_3 \cdot DMF$ (obbz = *N,N'*-Oxamidobis(benzoato) and DMF = Dimethylformamide), a Precursor of the Molecular-Based Magnet $MnCu(obbz) \cdot H_2O$ with T_c = 14 K

Francesc Lloret,*[1a] Miguel Julve,[1a] Rafael Ruiz,[1a] Yves Journaux,*[1b] Keitaro Nakatani,[1b] Olivier Kahn,*[1b] and Jorunn Sletten[1c]

Departament de Quimicà Inorgànica, Universitat de València, 46100-Burjassot (València), Spain, Department of Chemistry, University of Bergen, 5007 Bergen, Norway, and Laboratoire de Chimie Inorganique, Unité de Recherche Associée au CNRS No 420, Université de Paris-Sud, 91405 Orsay, France

Received April 17, 1992

After 3 years of efforts, we succeeded in obtaining single crystals of $MnCu(obbz)(H_2O)_3 \cdot DMF$ (**1**) (obbz = *N,N'*-oxamidobis(benzoato) and DMF = dimethylformamide). **1** is a precursor of the molecular-based magnet $MnCu(obbz) \cdot H_2O$ (**2**) exhibiting a spontaneous magnetization below T_c = 14 K. **1** crystallizes in the orthorhombic system, space group *Pbca*. The lattice parameters are *a* = 10.3006 (6) Å, *b* = 22.375 (2) Å, *c* = 19.639 (1) Å, and *Z* = 8 (MnCu units). The structure consists of alternating bimetallic chains running along the *c* axis, the Mn(II) and Cu(II) ions being alternately bridged by oxamido and carboxylato groups. The conformation around the carboxylato bridge is of the syn–anti type. The chains stack on top of one another along the *a* axis, and are separated by noncoordinated DMF molecules along the *b* axis. The magnetic susceptibility of **1**, investigated down to 2 K, is characteristic of one-dimensional ferrimagnetic behavior with a minimum in the $\chi_M T$ versus *T* curve at 35 K (χ_M is the molar magnetic susceptibility and *T* is the temperature). Two theoretical models have been used to interpret these data. Model 1 consists of treating $S_{Mn} = {}^5/_2$ as a classical spin and $S_{Cu} = {}^1/_2$ as a quantum spin, with two interaction parameters J_1 and J_2. This model might be of limited applicability in the case of **1**, due to the low value of the ratio J_2/J_1. Model 2 describes the system as consisting of chains of oxamido-bridged $Mn^{II}Cu^{II}$ units weakly coupled in a ferromagnetic fashion through carboxylato bridges. Knowing the crystal structure of **1**, it has been possible to propose a scheme describing the irreversible transformation from **1** to the molecular-based magnet **2**. In **2** each Mn(II) ion belonging to a chain would bind to two free carboxylato oxygen atoms belonging to the adjacent chains just above and below along the *a* axis, affording a two-dimensional network. The interplane interactions would be favored by the removal of the DMF molecules.

Introduction

Three years ago, we reported on the synthesis and the magnetic properties of two compounds arising from the reaction of the Mn(II) ion with the $[Cu(obbz)]^{2-}$ dianion

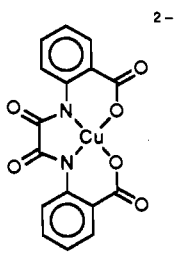

where obbz stands for *N,N'*-oxamidobis(benzoato). These compounds are $MnCu(obbz) \cdot 5H_2O$ and $MnCu(obbz) \cdot H_2O$.[2] The former phase shows the typical behavior of a one-dimensional ferrimagnet with a minimum at 44 K in the $\chi_M T$ versus T plot, χ_M being the molar magnetic susceptibility and T the temperature, and a sharp maximum at 2.3 K due to a three-dimensional magnetic ordering. In contrast, the latter compound exhibits a three-dimensional magnetic transition at T_c = 14 K with a spontaneous magnetization below T_c. In the magnetically ordered state the magnetization versus magnetic field curve shows a hysteresis loop characteristic of a soft magnet. When this result was published, $MnCu(obbz) \cdot H_2O$ had the highest ordering temperature ever reported for a molecular-based magnet. Later at least four other molecular magnets have been described with higher T_c's, namely (i) $[Mn(F_5benz)_2]_2NIT\text{-}Et$, where F_5benz is pentafluorobenzoato and NIT-Et an ethyl-substituted nitronyl nitroxide radical with T_c = 20.8 K;[3] (ii) $MnCu(pbaOH)(H_2O)_2$, where pbaOH stands for 2-hydroxy-1,3-propylenebis(oxamato) with T_c = 30 K;[4] (iii) $(tdae)_xC_{60}$, where tdae is tetrakis(dimethylamino)ethylene with T_c = 16.5 K;[5] (iv) and finally $V(TCNE)_2 \cdot nCH_2Cl_2$, where TCNE = tetracyanoethylene, the critical temperature of which is above 300 K.[6] Interestingly, in the first two compounds and probably also in the fourth one the nearest neighbor spin carriers are antiferromagnetically coupled, such that the spontaneous magnetization in the magnetically ordered state arises from a noncompensation of the magnetic moments.

In spite of many efforts neither the crystal structure of $MnCu(obbz) \cdot 5H_2O$ nor that of $MnCu(obbz) \cdot H_2O$ were known when we published our findings concerning these compounds. That is why we studied their XANES and EXAFS spectra at both Mn and Cu edges. These spectra are consistent with a basic structure of alternating bimetallic chains, with alternation of both the spin

(1) (a) Universitat de València. (b) Université de Paris-Sud. (c) University of Bergen.
(2) Nakatani, K.; Carriat, J. Y.; Journaux, Y.; Kahn, O.; Lloret, F.; Renard, J. P.; Pei, Y.; Sletten, J.; Verdaguer, M. *J. Am. Chem. Soc.* **1989**, *111*, 5739.
(3) Caneschi, A.; Gatteschi, D.; Renard, J. P.; Rey, P.; Sessoli, R. *J. Am. Chem. Soc.* **1989**, *111*, 785.
(4) Nakatani, K.; Bergerat, P.; Codjovi, E.; Mathonière, C.; Pei, Y.; Kahn, O. *Inorg. Chem.* **1991**, *30*, 3977.
(5) Allemand, P. M.; Khermani, K. C.; Koch, A.; Wudl, F.; Holczer, K.; Donovan, S.; Grüner, G.; Thompson, J. D. *Science* **1991**, *253*, 301.
(6) Manriquez, J. M.; Yee, G. T.; McLean, R. S.; Epstein, A. J.; Miller, J. S. *Science* **1991**, *252*, 1415.

0020-1669/93/1332-0027$04.00/0

carriers, Mn(II) and Cu(II), and interaction pathways, oxamido and carboxylato. A structural model was proposed.[2] It was assumed that, at least in the monohydrated phase, the chains were linked to each other, forming a two- or three-dimensional network. No additional detail was given concerning the association of chains.

Subsequently, in order to obtain information on the structure of compounds of the same family, we synthesized several species where $[Cu(obbz)]^{2-}$ was replaced by $[Cu(X_4obbz)]^{2-}$

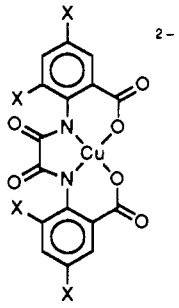

X = Cl or Br

When X = Br, an alternating bimetallic chain compound of formula $MnCu(Br_4obbz)(H_2O)_3 \cdot 2H_2O$ was structurally characterized;[7] it does not show any ferromagnetic transition, even after thermal treatment. Similarly, we replaced $[Cu(obbz)]^{2-}$ by $[Cu(obzp)]^{2-}$ (obzp = oxamido-*N*-benzoato-*N'*-propionato). The resulting compound, of formula $MnCu(obzp)(H_2O)_3 \cdot H_2O$, has the expected structure but behaves magnetically as isolated $Mn^{II}Cu^{II}$ pairs.[8,9] During all this time, we did not stop trying to get single crystals in the Mn(II)/$[Cu(obbz)]^{2-}$ system, and we recently succeeded, following a somewhat different synthetic route. The compound has the formula $MnCu(obbz)(H_2O)_3 \cdot DMF$ (**1**) with DMF = dimethylformamide. As $MnCu(obbz) \cdot 5H_2O$, **1** can be easily transformed into the molecular-based magnet $MnCu(obbz) \cdot H_2O$ (**2**). In this paper we describe the structure and the magnetic properties of **1**, and we discuss the probable mechanism leading from **1** to **2**. Finally we propose a structural model for **2**.

Experimental Section

Syntheses of 1 and 2. $Na_2[Cu(obbz)] \cdot 4H_2O$ was prepared as previously described.[2] **1** was synthesized as follows: a solution of 0.0724 g (0.2 mmol) of manganese(II) perchlorate hexahydrate in 20 mL of dimethylformamide (DMF) was added to a solution of 0.102 g (0.2 mmol) of $Na_2[Cu(obbz)] \cdot 4H_2O$ also dissolved in 20 mL of DMF. A few drops of water could be added into the former solution to facilitate the dissolution of the Mn(II) salt. Well-shaped single crystals of **1** were obtained by aerial diffusion of water in a closed container. The treatment of **1** under vacuum at room temperature, or at ambient pressure at 60 °C affords **2**. Anal. Calcd for $C_{19}H_{21}N_3O_{10}CuMn$ (**1**): C, 40.04; H, 3.71; N, 7.37; O, 28.07; Cu, 11.15; Mn, 9.64. Found: C, 40.50; H, 3.95; N, 7.87; O, 27.65; Cu, 11.10; Mn, 9.60. Calcd for $C_{16}H_{14}N_2O_7CuMn$ (**2**): C, 41.71; H, 2.19; N, 6.08; Cu, 13.79; Mn, 11.92. Found: C, 41.29; H, 2.86; N, 6.66; Cu, 13.70; Mn, 11.90. We confirmed that the X-ray powder pattern of **2** is strictly identical to that of the magnetic phase described in ref 2.

Crystallographic Data Collection and Structure Determination. All measurements were carried out at 294 K on an Enraf-Nonius CAD4 diffractometer using graphite-monochromated Mo Kα radiation (λ = 0.710 73 Å). A violet platelike crystal limited by faces {100}, {001}, and {010} and of size 0.26 × 0.18 × 0.07 mm was used for data collection. Cell parameters were determined from least-squares refinement of 25 well-centered reflections ($13° < 2\theta < 33°$). The crystal data are summarized in Table I; a full length table of crystallographic data is given in the supplementary material (Table SI). A total of 3529 unique reflections were recorded in the range $2° < 2\theta < 48°$ from the *hkl* octant. The intensities of three standard reflections measured every 2 h did not decline significantly. The random error in any one reflection is calculated as $\sigma_I = [\sigma_c^2 + (0.02F_0^2)^2]^{1/2}$. The data were corrected for Lorentz and polarization effects and for absorption by the Gaussian integration method. The structure was solved by direct methods and subsequent Fourier syntheses. In the course of this process it was found that one molecule of dimethylformamide per asymmetric unit was present in the crystal lattice. Refinement was performed with the full-matrix least-squares method. Hydrogen atoms, except in methyl groups, were located in a difference Fourier map, and were included in the refinement. The refinement based on 2368 reflections with $|F| > 2\sigma_F$ converged at R = 0.041, R_w = 0.037, and s = 1.68. The scattering curves, with anomalous dispersion terms included, were those of Cromer and Waber.[10] All calculations were carried out on a MICRO-VAXII computer using the Enraf-Nonius Structure Determination programs.[11] Parameters of non-hydrogen atoms are listed in Table II, and bond distances and angles for non-hydrogen atoms, in Tables III and IV. In the supplementary material parameters of hydrogen atoms, anisotropic thermal parameters, distances and angles involving hydrogen atoms, hydrogen bonds, and equations of least-squares planes are given (Tables SII–SVI).

Table I. Crystallographic Data for $MnCu(obbz)(H_2O)_3 \cdot DMF$ (**1**)

chem formula	$C_{19}H_{21}N_3O_{10}CuMn$
fw	569.87
space group	Pbca (No. 61)
a, Å	10.3006 (6)
b, Å	22.375 (2)
c, Å	19.639 (1)
V, Å^3	4526.2 (9)
Z	8
T, °C	21
λ, Å	0.710 73
ρ(calcd), g cm^{-3}	1.672
μ(Mo Kα), cm^{-1}	15.355
transm coeff	0.750–0.895
$R = \sum\|\|F_o\| - \|F_c\|\|/\sum\|F_o\|$	0.041
$R_w = \{\sum w(\|\|F_o\| - \|F_c\|\|)^2/\sum w\|F_o\|^2\}^{1/2}$ [a]	0.037

[a] $w = 1/\sigma_F^2$, $\sigma_F = \sigma_I(IL_p)^{-1/2}$; $\sigma_I = [\sigma_c^2 + (0.002N_{net})^2]^{1/2}$, where N_{net} is the net count of each reflection.

Description of the Structure of $MnCu(obbz)(H_2O)_3 \cdot DMF$ (1)

The structure of **1** consists of alternating bimetallic chains running along the *c* axis with Mn(II) and Cu(II) ions bridged by oxamido (Mn···Cu = 5.483 (1) Å) and carboxylato (Mn···Cu = 4.608 (1) Å) groups. The conformation around the carboxylato bridge is of the syn–anti type. Each unit along the chain is symmetry related to its neighbor by the 2-fold screw axis. Two asymmetric units along a chain are depicted in Figure 1, which also shows the atomic numbering scheme. The copper atom binds to both of the oxamido nitrogen atoms and to an oxygen atom from each of the two carboxylato groups. The coordination is square planar with a small tetrahedral distortion. The ligand atoms deviate by ±0.083 Å and the copper atom by 0.053 Å from a least-squares plane defined by the ligand atoms. The manganese atom binds to both of the oxamido oxygen atoms, a carboxylato oxygen atom, and three water molecules in a distorted octahedral geometry. The distortion is related to the fact that the atom O4 of the carboxylato bridge is situated only 2.89 Å from Mn and to the existence of an intrachain hydrogen bond O9···O3 ($^1/_2 - x, 1 - y, ^1/_2 + z$) = 2.712 Å. Two Mn–O bond lengths involving water molecules are significantly longer (Mn–O7 = 2.193 Å; Mn–O8 = 2.208 Å) than the third one (Mn–O9 = 2.111 Å). The dihedral angle between the Mn equatorial plane (defined by O1, O2, O9, and O6 ($^1/_2 - x, 1 - y, ^1/_2 + z$)) and the Cu equatorial plane across the oxamide bridge is 1.8° and that across the carboxylate bridge is 3.5°.

(7) Nakatani, K.; Sletten, J.; Halut-Desporte, S.; Jeannin, S.; Jeannin, Y.; Kahn, O. *Inorg. Chem.* **1991**, *30*, 164.
(8) Pei, Y.; Nakatani, K.; Kahn, O.; Sletten, J.; Renard, J. P. *Inorg. Chem.* **1989**, *28*, 3170.
(9) Kahn, O.; Pei, Y.; Nakatani, K.; Journaux, Y.; Sletten, J. *New J. Chem.* **1992**, *16*, 269.
(10) Cromer, D. T.; Waber, J. T. *International Tables for X-Ray Crystallography*; Kynoch Press: Birmingham, England, 1974; Vol. IV, p 99, Table 2.2B.
(11) Frez, B. A. *The SDP-User's Guide*, (*SDPVAX V.3*); Enraf Nonius: Delft, The Netherlands, 1985.

Table II. Atomic Parameters for MnCu(obbz)(H2O)3 (1)

atom	x	y	z	B_{eq},[a] Å²
Cu	0.29719 (6)	0.54498 (3)	0.22054 (3)	2.43 (1)
Mn	0.26677 (7)	0.50632 (4)	0.49578 (4)	2.27 (1)
O1	0.3848 (3)	0.5515 (2)	0.4151 (2)	2.52 (8)
O2	0.1914 (4)	0.4773 (2)	0.3975 (2)	2.89 (8)
O3	0.4217 (4)	0.5819 (2)	0.1614 (2)	2.88 (8)
O4	0.2152 (4)	0.5143 (2)	0.1408 (2)	3.19 (8)
O5	0.6020 (4)	0.6268 (2)	0.1299 (2)	2.99 (8)
O6	0.1202 (3)	0.4496 (2)	0.0752 (2)	2.62 (8)
O7	0.3981 (3)	0.4293 (2)	0.5010 (2)	3.12 (8)
O8	0.1450 (3)	0.5875 (2)	0.4960 (2)	2.96 (8)
O9	0.1053 (3)	0.4574 (2)	0.5316 (2)	3.71 (9)
N1	0.3762 (4)	0.5780 (2)	0.3010 (2)	1.92 (9)
N2	0.1889 (4)	0.4985 (2)	0.2810 (2)	2.06 (8)
C1	0.3405 (5)	0.5483 (2)	0.3558 (2)	2.1 (1)
C2	0.2299 (5)	0.5039 (2)	0.3451 (2)	2.1 (1)
C3	0.4686 (5)	0.6248 (2)	0.3031 (2)	2.3 (1)
C4	0.5396 (5)	0.6403 (2)	0.2438 (3)	2.2 (1)
C5	0.5212 (5)	0.6141 (2)	0.1742 (2)	2.5 (1)
C6	0.6323 (6)	0.6857 (3)	0.2497 (3)	3.6 (1)
C7	0.6510 (7)	0.7167 (3)	0.3092 (3)	4.4 (2)
C8	0.5780 (7)	0.7041 (3)	0.3658 (3)	3.9 (1)
C9	0.4886 (6)	0.6592 (3)	0.3620 (3)	3.1 (1)
C10	0.0902 (5)	0.4581 (2)	0.2621 (2)	2.0 (1)
C11	0.0715 (5)	0.4420 (2)	0.1932 (2)	2.2 (1)
C12	0.1407 (5)	0.4704 (2)	0.1342 (2)	2.3 (1)
C13	−0.0205 (6)	0.3986 (3)	0.1767 (3)	3.5 (1)
C14	−0.0970 (6)	0.3729 (3)	0.2253 (3)	4.3 (1)
C15	−0.0856 (6)	0.3907 (3)	0.2928 (3)	3.6 (1)
C16	0.0064 (6)	0.4324 (3)	0.3111 (3)	3.0 (1)

[a] Values for anisotropically refined atoms are given in the form of the isotropic equivalent thermal parameter defined as $B_{eq} = (4/3)\sum_i\sum_j\beta_{ij}a_ia_j$.

Table III. Bond distances (Å) Involving Non-Hydrogen Atoms for MnCu(obbz)(H2O)3·DMF (1)[a]

Cu–O3	1.917 (3)	N2–C10	1.410 (5)
Cu–O4	1.908 (3)	N3–C17	1.290 (8)
Cu–N1	1.924 (3)	N3–C18	1.453 (7)
Cu–N2	1.933 (3)	N3–C19	1.449 (8)
Mn–O1	2.239 (3)	C1–C2	1.526 (6)
Mn–O2	2.179 (3)	C3–C4	1.418 (6)
Mn–O6[1]	2.182 (3)	C3–C9	1.405 (6)
Mn–O7	2.193 (4)	C4–C5	1.499 (6)
Mn–O8	2.208 (4)	C4–C6	1.400 (6)
Mn–O9	2.111 (4)	C6–C7	1.372 (7)
O1–C1	1.252 (4)	C7–C8	1.371 (7)
O2–C2	1.253 (4)	C8–C9	1.365 (7)
O3–C5	1.278 (5)	C10–C11	1.413 (5)
O4–C12	1.252 (5)	C10–C16	1.414 (6)
O5–C5	1.237 (5)	C11–C12	1.503 (6)
O6–C12	1.266 (5)	C11–C13	1.395 (6)
O10–C17	1.257 (8)	C13–C14	1.366 (7)
N1–C1	1.318 (5)	C14–C15	1.390 (7)
N1–C3	1.415 (5)	C15–C16	1.377 (6)
N2–C2	1.344 (5)		

[a] Symmetry operation 1; $^1/_2 - x$, $1 - y$, $^1/_2 + z$.

The crystal packing is shown in Figure 2. The shortest interchain metal···metal distances involve metal ions of the same nature and occur between chains stacked on top of one another along the *a* axis. The corresponding distances are Mn···Mn ($1 - x$, $1 - y$, $1 - z$) = 4.816 Å, Cu···Cu ($^1/_2 + x$, y, $^1/_2 - z$) = 5.279 Å, and Mn···Mn ($-x$, $1 - y$, $1 - z$) = 5.506 Å. The shortest distances between the stacks of chains are Cu···Mn ($^1/_2 + x$, y, $^1/_2 - z$) = 6.496 Å and Cu···Mn ($-^1/_2 + x$, y, $^1/_2 - z$) = 6.975 Å. The chains within each stack are also connected through hydrogen bonding (see Table SVI). Neighboring stacks are separated by dymethylformamide molecules.

Magnetic Properties of MnCu(obbz)(H2O)3·DMF (1)

The magnetic behavior of **1** is represented in Figure 3 in the form of the $\chi_M T$ versus T plot. At room temperature $\chi_M T$ is equal to 4.41 cm³ K mol⁻¹, a value which is very slightly smaller than that expected for uncoupled Mn(II) and Cu(II) ions. $\chi_M T$ decreases as T is lowered, reaches a minimum around 35 K, with $\chi_M T$ = 3.42 cm³ K mol⁻¹, and finally increases again as T is lowered further down to 2 K. At this temperature $\chi_M T$ is found to be equal to 15.14 cm³ K mol⁻¹ and presents a sharp maximum, due to three-dimensional antiferromagnetic ordering. This behavior is rather similar but not strictly identical to that of MnCu(obbz)·5H2O. To interpret these data we used two models, hereafter noted as model 1 and model 2.

Table IV. Bond Angles (deg) Involving Non-Hydrogen Atoms for MnCu(obbz)(H2O)3·DMF (1)

O3–Cu–O4	87.4 (1)	O1–C1–N1	129.0 (4)
O3–Cu–N1	92.8 (1)	O1–C1–C2	115.9 (4)
O3–Cu–N2	171.9 (1)	N1–C1–C2	115.1 (8)
O4–Cu–N1	178.2 (1)	O2–C2–N2	129.2 (4)
O4–Cu–N2	93.1 (1)	O2–C2–C1	115.6 (3)
N1–Cu–N2	87.0 (1)	N2–C2–C1	115.2 (3)
O1–Mn–O2	72.6 (1)	N1–C3–C4	120.2 (4)
O1–Mn–O6[1]	90.7 (1)	N1–C3–C9	121.9 (4)
O1–Mn–O7	93.0 (2)	C4–C3–C9	117.8 (4)
O1–Mn–O8	86.5 (1)	C3–C4–C5	126.1 (4)
O1–Mn–O9	153.8 (1)	C3–C4–C6	117.4 (4)
O2–Mn–O6[1]	163.3 (1)	C5–C4–C6	116.4 (4)
O2–Mn–O7	91.6 (2)	O3–C5–O5	122.1 (4)
O2–Mn–O8	92.6 (1)	O3–C5–C4	120.0 (4)
O2–Mn–O9	81.9 (1)	O5–C5–C4	117.8 (4)
O6[1]–Mn–O7	89.6 (1)	C4–C6–C7	122.3 (5)
O6[1]–Mn–O8	85.9 (1)	C6–C7–C8	120.3 (5)
O6[1]–Mn–O9	114.6 (1)	C7–C8–C9	118.5 (5)
O7–Mn–O8	175.5 (2)	C3–C9–C8	123.2 (5)
O7–Mn–O9	93.6 (2)	N2–C10–C11	120.8 (4)
O8–Mn–O9	88.7 (2)	N2–C10–C16	121.5 (3)
Cu–O3–C5	131.4 (3)	C11–C10–C16	117.7 (4)
Cu–O4–C12	129.7 (3)	C10–C11–C12	124.5 (4)
Mn–O6[1]–C12[1]	113.5 (3)	C10–C11–C13	119.5 (4)
Cu–N1–C1	111.0 (3)	C12–C11–C13	115.9 (4)
Cu–N1–C3	126.4 (3)	O4–C12–O6	119.1 (4)
C1–N1–C3	122.4 (3)	O4–C12–C11	122.8 (4)
Cu–N2–C2	110.4 (3)	O6–C12–C11	118.1 (4)
Cu–N2–C10	126.9 (2)	C11–C13–C14	121.5 (5)
C2–N2–C10	122.3 (3)	C13–C14–C15	119.8 (5)
C17–N3–C18	124.8 (7)	C14–C15–C16	120.1 (5)
C17–N3–C19	120.7 (6)	C10–C16–C15	121.2 (4)
C18–N3–C19	114.5 (6)	O10–C17–N3	125.8 (7)

Model 1. The spin Hamiltonian taking into account the Zeeman perturbation is written as

$$H = -J\sum_i \mathbf{S}_{Cu,i}[(1+\alpha)\mathbf{S}_{Mn,i} + (1-\alpha)\mathbf{S}_{Mn,i+1}] + \sum_i (g_{Cu}\mathbf{S}_{Cu,i} + g_{Mn}\mathbf{S}_{Mn,i})\beta H \quad (1)$$

i runs over the MnCu units. $\mathbf{S}_{Mn,i}$ and $\mathbf{S}_{Cu,i}$ are local spin operators; the former are treated as classical spins and the latter as quantum spins. H is the applied magnetic field. Each Cu(II) ion interacts with two nearest-neighbor Mn(II) ions, the interaction parameters being $J(1 + \alpha)$ and $J(1 - \alpha)$, respectively. g_{Cu} and g_{Mn} are the local g factors assumed to be isotropic. The equations leading to the theoretical variation of χ_M have been given elsewhere.[2,9] The least-squares fitting of the experimental data leads to J = −7.8 cm⁻¹, α = 0.79, g_{Mn} = 1.98, and g_{Cu} = 2.10. The agreement factor defined as $R = \sum[(\chi_M T)^{obs} - (\chi_M T)^{calc}]^2/\sum[(\chi_M T)^{obs}]^2$ is then equal to 2.2×10^{-4}. The two exchange parameters between Mn(II) and Cu(II) nearest-neighbor ions are therefore $J_1 = J(1 + \alpha)$ = −14 cm⁻¹ and $J_2 = J(1 - \alpha)$ = −1.7 cm⁻¹. The oxamido bridge is known to propagate a rather strong antiferromagnetic interaction. Therefore the J_1 parameter is clearly associated with the interaction through oxamido, and J_2 is clearly associated with the interaction through carboxylato. In all oxamido-bridged Mn^{II}-Cu^{II} compounds described so far the interaction parameter through oxamido has a value around −28 cm⁻¹. No structural modification can justify the fact that in **1** the interaction would be much smaller (in absolute value). The discrepancy between the calculated value of J_1 in this model and the values already reported in similar compounds strongly suggests that model 1 is not perfectly valid

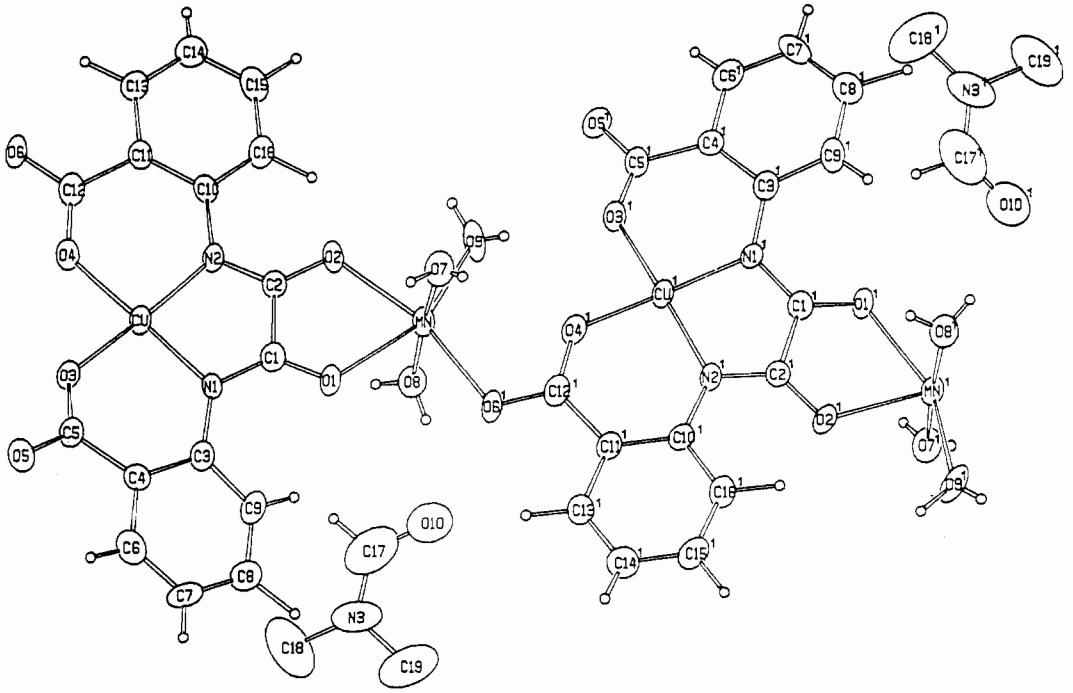

Figure 1. Section of single chain for **1** showing the atomic numbering scheme used. Thermal ellipsoids of non-hydrogen atoms are plotted at the 50% probability level. Hydrogen atoms are given an arbitrary radius.

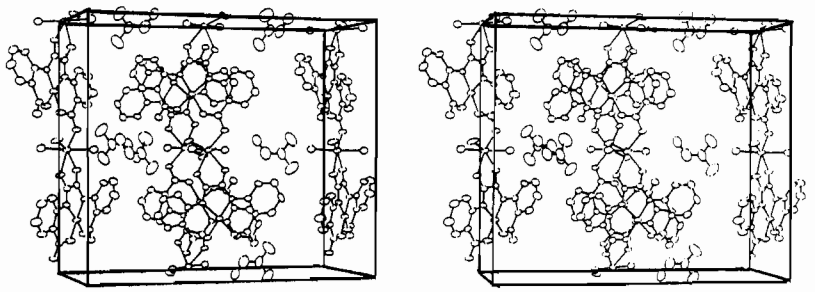

Figure 2. Stereodrawing showing crystal packing. The origin of the unit cell is in the lower left-hand corner, the *b* axis runs horizontally, and the *a* axis points toward the viewer.

in the present case (vide infra). The very weak value of J_2 is due to the syn–anti coordination round the carboxylato bridge.

Model 2. It has been stated[9] that model 1 fails when α is too close to 1. This can be easily shown when considering the limit case, $\alpha = 1$. Model 1 then leads to a low-temperature limit $(\chi_M T)_{LT}$ = 3.27 cm^3 K mol^{-1} (for $g_{Mn} = g_{Cu} = 2.00$). In fact, when α is equal to 1, J_2 is zero, and the system reduces to antiferromagnetically coupled $Mn^{II}Cu^{II}$ pairs with a J_1 interaction parameter. The low-temperature limit $(\chi_M T)_{LT}$ is reached when only the quintet ground state is thermally populated; it is equal to $2N\beta^2g^2/k$, i.e. 3.00 cm^3 K mol^{-1} (with $g = 2$).

The fitting of the experimental data with model 1 leads to α = 0.79 with an unreasonable J_1 value. If we impose $J_1 = -28$ cm^{-1}, α is found to be larger than 0.9, and the validity, or at least the accuracy, of model 1 in the present case is questionable. That is why we decided to test an alternative model. We describe the system as consisting of chains of oxamido-bridged $Mn^{II}Cu^{II}$ units denoted as P ferromagnetically coupled through the carboxylato bridges, which affords a ferromagnetic chain of P units. The spin S_P of the P unit depends on the J_1/kT ratio through the implicit equation

$$S_P(S_P + 1) = 6[5 + 14 \exp(3J_1/kT)]/[5 + 7 \exp(3J_1/kT)] \quad (2)$$

Equation 2 implicitly supposes that the g_{Mn} and g_{Cu} factors are equal. The low- and high-temperature limits of S_P are 2 and $^5/_2$, respectively. Whatever the temperature may be, S_P is large enough to be treated as a classical spin. The magnetic susceptibility per P unit for the ferromagnetic chain is then given by the classical spin model derived by Fisher as[12]

$$\chi_M = \frac{Ng^2\beta^2 S_P(S_P + 1)}{3kT} \frac{1 + u}{1 - u} \quad (3)$$

with

$$u = \coth [J_{eff}S_P(S_P + 1)/kT] - kT/S_P(S_P + 1) \quad (4)$$

g_P in (3) stands for the g factor of P. J_{eff} in (4) is the effective interaction parameter describing the magnitude of the ferromagnetic interaction between P units. Reporting $S_P(S_P + 1)$ from (2) into (3) and (4) leads to an expression of χ_M depending on J_1, J_{eff}, and g_P. Least-squares fitting of the experimental data yields $J_1 = -32$ cm^{-1}, $J_{eff} = 0.4$ cm^{-1}, and $g_P = 1.99$. The agreement factor R defined as above is equal to 8.1×10^{-5}, i.e. significantly smaller than in model 1. In model 2 the J_1 value agrees with the values found in other oxamido-bridged $Mn^{II}Cu^{II}$ pairs. The J_{eff} value confirms that the interaction between the oxamido-bridged $Mn^{II}Cu^{II}$ pairs through the carboxylato bridge is weak but not negligible. Model 2 seems to be more appropriate in the limit where the ratio J_2/J_1 is very small. In a certain sense this model corresponds to a perturbational approach; the magnetic behavior arising from the dominant interaction J_1 within the P pairs is slightly perturbed by the weak interpair interaction J_2. As a

(12) Fisher, M. E. *Am. J. Phys.* **1964**, *32*, 343.

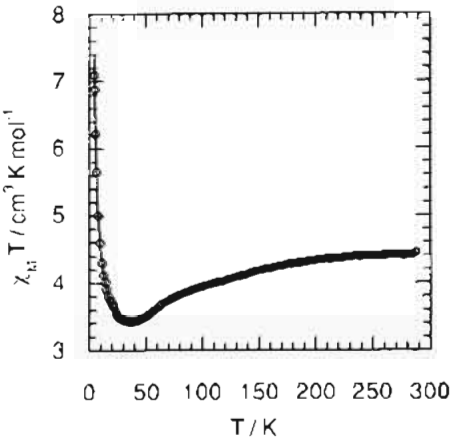

Figure 3. $\chi_M T$ versus T plot for MnCu(obbz)$(H_2O)_3$·DMF (1).

consequence of this, the validity of this model 2 is expected to decrease as α decreases with respect to unity. We intend to look for the α_0 value such that model 1 is more appropriate for $\alpha < \alpha_0$, and model 2 for $\alpha > \alpha_0$. It is worth mentioning that Gatteschi and co-workers used an approach rather similar to model 2 to fit the magnetic data of $Mn(hfa)_2(NIT\text{-}py)_2$ (hfa = hexafluoroacetylacetonato and NIT-py = pyridine-substituted nitronyl nitroxide radical).[13]

The magnetic properties of the molecular-based magnet **2** have been described in detail in ref 2.

Discussion and Conclusion

A prerequisite to understanding the mechanism affording a molecular-based magnet behavior is to have information on the three-dimensional structure of the compound. That is why we spent so much time to get single crystals of **2** and of its precursor MnCu(obbz)·$5H_2O$. Actually, we obtained a new phase, **1**, of the precursor, in which two noncoordinated water molecules are replaced by a DMF molecule.

The first information arising from this work is that the structure of **1** confirms the model that we had proposed from the XANES and EXAFS spectra; the structure of **1** consists of alternating bimetallic chains. The X-ray diffraction study brings also new insights on this structure. The conformation around the carboxylato bridge is of the syn–anti type as in MnCu(obzp)-$(H_2O)_3$·H_2O and MnCu(Br_4obbz)$(H_2)_3$·$2.5H_2O$. In contrast, the conformation is of the anti–anti type in MnCu(obp)$(H_2O)_3$·H_2O.[14] From the available structural and magnetic data, it had been stated that the interaction through the carboxylato bridge was negligible when the conformation was syn–anti and nonnegligible when it was anti–anti. The present results incite us to modify somewhat this statement. The J_2 interaction parameter through the carboxylato bridge in **1** is weak but not negligible. Otherwise, $\chi_M T$ would not increase as T is lowered below 35 K. The weak coupling through the carboxylato may be attributed to the fact that the Mn–carboxylato–Cu network in **1** is more planar than in the other compounds of the same kind with a syn–anti conformation. The J_2 parameter, however, cannot be determined accurately. Indeed, the mathematical model describing the magnetic properties of an alternating bimetallic chain compound fails when the ratio between the two interaction parameters becomes too small, which is the case for **1**. It seems more appropriate to describe the system as consisting of chains of ferromagnetically coupled units P, each unit being an oxamido-bridged $Mn^{II}Cu^{II}$ pair.

The crucial question concerns the structural modification accompanying the transformation of **1** into **2**. Under vacuum at ambient temperature, or under ambient pressure at 60 °C, not only the noncoordinated dimethylformamide molecule but also two of the three water molecules bound to the Mn(II) ion in **1** are removed. The structural data strongly suggest that the two Mn–O bonds which are broken are Mn–O7 and Mn–O8. Indeed, the corresponding Mn–O bond lengths are significantly longer than Mn–O9. Moreover, the water molecule involving O9 seems to be stabilized by the intrachain Mn···O3 ($^1/_2 - x$, $1 - y$, $^1/_2 + z$) hydrogen bond. The XANES data unambiguously indicate that the Mn(II) ion possesses an octahedral environment of oxygen atoms both in **1** and **2**. This apparently is possible only if this ion binds to two carboxylato oxygen atoms belonging to adjacent chains in **2**, resulting in a two- or three-dimensional network. Interestingly, two of the interchain separations between the Mn(II) ion and carboxylato oxygen atoms in **1** are very short, namely Mn···O5 ($-^1/_2 + x$, y, $^1/_2 - z$) = 4.033 Å and Mn···O6 ($^1/_2 + x$, y, $^1/_2 - z$) = 4.100 Å. Those separations involve chains stacking along the a axis. It might be also worthwhile to point out that the hydrogen bonds O7 (x, y, z)···O6 ($^1/_2 + x$, y, $^1/_2 - z$) = 2.77 Å and O8 (x, y, z)···O5 ($-^1/_2 + x$, y, $^1/_2 - z$) = 2.66 Å in **1** occur between the Mn axial water molecules and the carboxylato oxygen atoms in the adjacent chains. Those data lead us to propose the following process for the transformation from **1** to **2**: the two water molecules involving the O7 and O8 atoms are removed, and instead Mn(II) binds to the carboxylato oxygen atoms O5 and O6 belonging to the adjacent chains just above and just below, respectively, along the a axis, affording a two-dimensional network with planes parallel to ac. Furthermore the removal of the DMF molecules favors the interplane interactions along the b axis. A schematic representation of this postulated two-dimensional structure is shown in Figure 4. Thermodynamically, the molecular magnet **2** is more stable than **1**. As a matter of fact, the transformation **1** → **2** is irreversible. A rather similar polymerization reaction in the solid state affording a molecular-based magnet has been found for MnCu(obze)$(H_2O)_4$.[15] In this latter case, however, the structure of the precursor consists of isolated $Mn^{II}Cu^{II}$ dinuclear units instead of bimetallic chains.

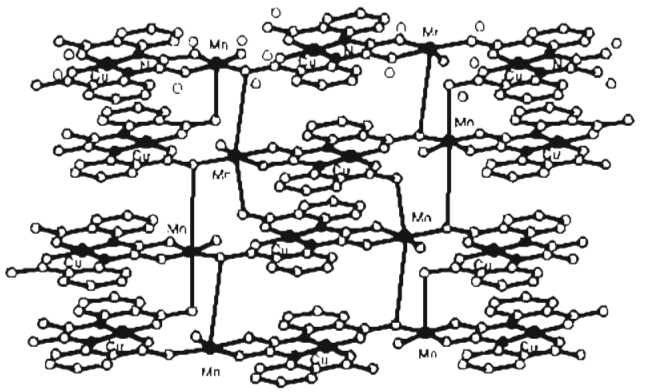

Figure 4. Schematic representation of the two-dimensional structure postulated for the molecular-based magnet MnCu(obbz)·H_2O (2) (see text). For clarity, the Mn–O(carboxylato) bonds have been lengthened.

Supplementary Material Available: Tables SI–SVII, listing detailed crystallographic data, crystallographic parameters for hydrogen atoms, anisotropic thermal parameters for non-hydrogen atoms, bond distances and angles involving hydrogen atoms, hydrogen bonds, and least-squares planes and dihedral angles, respectively (8 pages). Ordering information is given on any current masthead page.

(13) Caneschi, A.; Ferraro, F.; Gatteschi, D.; Rey, P.; Sessoli, R. *Inorg. Chem.* **1990**, *29*, 4217.
(14) Pei, Y.; Kahn, O.; Sletten, J.; Renard, J. P.; Georges, R.; Gianduzzo, J. C.; Curely, J.; Xu, Q. *Inorg. Chem.* **1988**, *27*, 47.
(15) Pei, Y.; Kahn, O.; Nakatani, K.; Codjovi, E.; Mathonière, C.; Sletten, J. *J. Am. Chem. Soc.* **1991**, *113*, 6558.